Chapter 7
Application of ReaxFF-Reactive Molecular Dynamics and Continuum Methods in High-Temperature/Pressure Pyrolysis of Fuel Mixtures

Chowdhury Ashraf, Sharmin Shabnam, Yuan Xuan and Adri C. T. van Duin

Abstract Rocket engines, gas turbines, HCCI engines, and other such combustion devices frequently exceed the critical pressure of the fuel or the oxidizer. Modeling of combustion processes at high-pressure operating condition is required to determine the reaction rates based on which chemical kinetic models are developed. The current need is to focus on the transfer from low pressure to high-pressure conditions as this can have a significant effect on the chemistry as well as the reaction rates. The ReaxFF reactive force field method is a computationally feasible method used to study the combustion kinetics of fuels and fuel mixtures at supercritical condition. In this chapter, ReaxFF-MD is used to investigate the effect of a highly reactive fuel on the properties of a less reactive fuel at different levels of concentration, temperature, and density/pressure. The activation energies, based on Arrhenius-type rate laws, are compared with those from Continuum simulations and the limitations of the latter has been elaborated on. The study reveals a pressure/temperature regime and mixing conditions, where simple first-order kinetics-based Arrhenius-type relations cannot be applied. The reason can be attributed to different initial reaction mechanisms and product distributions of the two fuels considered. These results indicate how ReaxFF-based molecular dynamics simulations can provide significant atomistic insights on the combustion properties of fuel mixtures at supercritical conditions, where experiments are difficult to perform.

Keywords Pyrolysis · Arrhenius parameters · Fuel mixture · Toluene · n-Dodecane

Chowdhury Ashraf and Sharmin Shabnam have contributed equally to this manuscript.

C. Ashraf · S. Shabnam · Y. Xuan · A. C. T. van Duin (✉)
Department of Mechanical Engineering, The Pennsylvania State University, State College, PA, USA
e-mail: acv13@psu.edu

N. Goldman (ed.), *Computational Approaches for Chemistry Under Extreme Conditions*, Challenges and Advances in Computational Chemistry and Physics 28,
https://doi.org/10.1007/978-3-030-05600-1_7

7.1 Introduction

Many combustion devices such as rocket, gas turbines, diesel, and HCCI engines achieve an operating pressure, which is much higher than the critical pressure of either the fuel or the oxidizer. For example, rocket engines using H_2 as fuel can achieve a pressure excess of 100 atm [1], while the critical pressure of the fuel (H_2) and oxidizer (O_2) is 13 atm and 50 atm, respectively [2]. Similarly, pressure inside the combustion chamber of diesel engine increases from ~25 atm during injection to 60 atm [3, 4] after ignition, which is beyond the critical pressure of any of the components of diesel fuels. The physical and the chemical mechanisms of combustion at this pressure/temperature condition is drastically different than its low-pressure counterpart, since molecules are densely packed and may experience van der Waals interactions and caging effects under high pressure [5]. Therefore, a detailed understanding of this complex process is important for the further development of these devices.

When a fuel is sprayed into the combustion chamber, it mixes with a stream of high-pressure fluid, which is primarily the oxidizer. This molecular mixing process has a great influence on autoignition and is a strong precursor of combustion. Additionally, during combustion, the heavier fuel species first undergo chemical decomposition, i.e., pyrolysis and then oxidation. Due to the nonuniform nature of the combustion (both pyrolysis and oxidation) reactions, highly active and fast moving radicals are generated in one location and mix with fuel and oxidizer at a different location inside the combustion chamber and significantly alter the combustion dynamics. Thus, this turbulent mixing of multiple chemical species under high pressure conditions has been an active area of research for the combustion community. However, despite this great interest, the experimental studies [6–12] are limited to only single or binary species mixing instead of multicomponent mixing. Additionally, most studies are based on qualitative visualization with rare quantitative analysis due to the difficulties of performing experiments at supercritical conditions, and therefore cannot be used to validate the proposed kinetic models at high-pressure conditions. Furthermore, these studies except a few [6, 13, 14] have used simple species like N_2, H_2, and O_2 in their turbulent mixing study, which require very simple chemical kinetic models, whereas the real fuels used inside combustion chambers are rather complex ones.

Since the experiments fail to provide sufficient information regarding the complex physical (diffusion, turbulence) and chemical (reaction) coupling of turbulent mixing, computational fluid dynamics (CFD) simulations have emerged as a potential solution to study most of the physical aspects of these problems. Among different CFD techniques available, direct numerical simulation (DNS) has proved to be a powerful tool of combustion and turbulence research [15], since it can resolve any length and timescales of the flow using high order accurate methods. Masi et al. [16] have developed a DNS model to describe the multi- species high-pressure turbulence mixing. Combining this model with the rate of single-step chemical reaction consistent with ignition prediction [17], Jossette Bellan from Jet Propulsion Lab

(JPL) has recently studied both the diffusion [18] and turbulent reaction rate [19] of high pressure mixing. Additionally, Gnanaskandan et al. [5] studied the length of the potential core of round fluid jet entering high-pressure chamber using both DNS and large eddy simulations (LES) methods, and Foster et al. [20] studied the effect of Soret and Dufor cross diffusions in turbulent mixing. The pressure considered in these studies typically ranges from 60 to 100 atm.

All the CFD studies mentioned above mainly focused on the physical aspects of turbulent chemistry; their chemical model was fairly simplistic. For example, Bellan and coworkers [16, 18, 19] only considered single-step chemical reaction for n-heptane oxidation, while Foster et al. [20] considered very simple 7-step 10 species reduced mechanism for a similar problem. However, as mentioned above, a highly coupled relation between chemical and physical properties governs the turbulent mixing phenomenon, which cannot be fully captured by the simple chemical kinetic model.

Chemical kinetics models for various hydrocarbons are well documented in the literature [21]. However, these models are only developed for low-pressure/temperature condition. Additionally, these models were developed only considering temperature dependence on the reaction rates via simple Arrhenius-type rate laws, while neglecting pressure dependence on combustion pathways; which can significantly alter the chemical properties at high pressure. As experiments are difficult to be conducted at supercritical pressure and temperature, we need a computationally feasible method, which can simulate complex combustion reactions without requiring any user input of possible reactions; so that the complete reaction network can be captured. Quantum mechanical (QM)-based ab initio methods are the best choice for accurately predicting the reactions for such systems, however, they have serious system size and simulation time limitation [22]. Since these methods solve the Schrodinger equation to estimate reaction energies and barriers, they can only be applied to small systems typically containing a couple of hundred of atoms for a shorter time scale [22]. Recently, ReaxFF reactive force field method [23] has proven to be a useful alternative of QM-based methods for combustion chemistry simulations [24–31] as it can simulate larger systems for a longer time scale.

The focus of this book chapter is to demonstrate how the ReaxFF reactive force field method can be used as a valuable tool to study combustion kinetics of fuels and fuel mixtures at supercritical condition. The chapter is organized as follows: in Sect. 7.2, we will introduce the ReaxFF method itself while mentioning some of its previous applications in combustion study. In Sect. 7.3, we will elaborate on our systems and simulation setup. Next, some observations on combustions kinetics based on our simulations will be made in Sect. 7.4; and results obtained from ReaxFF simulations will be compared with continuum simulations. Lastly, we will provide some concluding remarks mentioning the pros and cons of ReaxFF simulation for studying similar problems and challenges and opportunities regarding the development of a multiscale ReaxFF/continuum simulation capability for high-temperature/high-density pyrolysis and combustion simulations.

7.2 ReaxFF Background

Since force field based methods are computationally inexpensive and can provide a reasonable agreement with quantum mechanical simulations, they are now being used extensively to get an atomistic insight of complex physical and chemical problems. While potentials such as DREIDING [32], MM [3, 33–35], MM [4, 36] COMPASS [37], etc., have been used to perform atomistic scale simulations of hydrocarbon fuels, mostly to study their thermodynamic properties, due to their rigid connectivity requirement they cannot be used to simulate chemical reactions. However, potentials such as first-[38] and second-generation [39] reactive empirical bond order (REBO), charge-optimized many-body (COMB) potential [40, 41], modified embedded atom method (MEAM) [42] and reactive force field (ReaxFF) [23] can dynamically simulate bond formation and bond breaking and capture chemical reactions. In this chapter, we will keep our discussion limited to the ReaxFF method and its application to high-pressure combustion.

ReaxFF adopts the concept of bond order introduced by Tersoff [43] and Brenner [38] and calculates the bond order of every pair of atoms as a function of their interatomic distances. Based on a certain cutoff value, ReaxFF finds the connectivity between atoms at each step, which enables ReaxFF to simulate dynamic bond breaking and bond formation during simulation. All the connectivity-dependent terms like bond, angle, and torsion energies are calculated based on bond order, thus nonbonded atom pairs do not contribute to these partial energies. Long-range interactions like van der Waals and Coulomb are not connectivity dependent and calculated between every pair of atoms, any excessive short-range nonbonded interactions are avoided by including a shielding term. ReaxFF calculates atomic charges using a geometry-dependent charge calculation scheme and uses electronegativity equalization method (EEM) [44] for this purpose. Additionally, for long-range interactions ReaxFF uses a cutoff distance (which is typically set to 10 Å) to reduce the computational cost. To eliminate any energy discontinuity and reduce the range of the Coulomb interactions, a seventh-order Taper function is employed [23]. Equation (7.1) shows the different energy components of ReaxFF total energy, while Fig. 7.1 demonstrates the complicated internal scheme of ReaxFF. A more detailed description of the ReaxFF energy terms can be found in the previous literature [23, 24].

$$E_{\text{system}} = E_{\text{bound}} + E_{\text{over}} + E_{\text{under}} + E_{\text{lp}} + E_{\text{val}} + E_{\text{tor}} + E_{\text{vdWaals}} + E_{\text{coulomb}} \quad (7.1)$$

where E_{bond}, E_{over}, $E_{\text{under,}}$ E_{lp}, E_{val}, E_{tor}, E_{vdWaals}, E_{coulomb} represent bond energy, over-coordination energy penalty, under-coordination stability, lone pair energy, valence angle energy, torsion angle energy, van der Waals energy, and coulomb energy, respectively.

ReaxFF force field parameters are trained against QM-calculations in describing energies and barriers for chemical reactions while solving Newton's equation of motion to generate a dynamic description of complex reactive systems. Thus, ReaxFF-based molecular dynamics (MD) simulations are a number of magnitudes

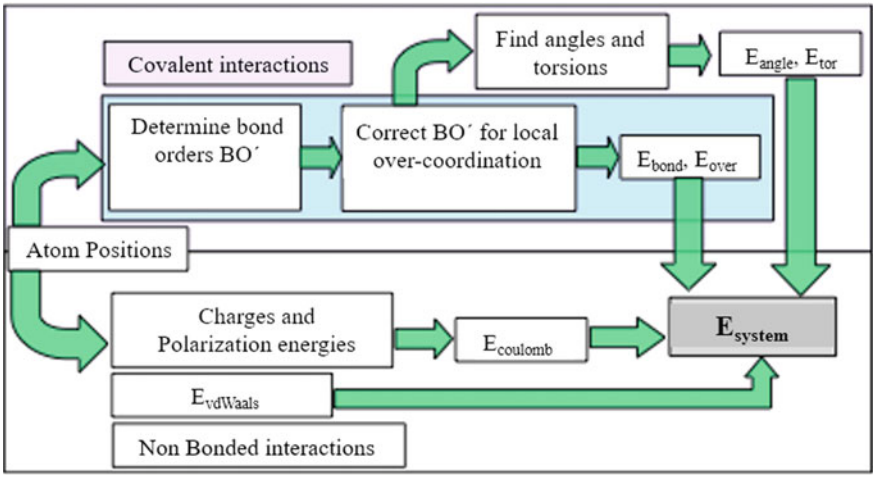

Fig. 7.1 Internal scheme of ReaxFF

faster than QM-based simulations while approaching the accuracy of those methods. Additionally, the inclusion of polarizable charge description and bond-order-dependent 3- and 4-body terms in ReaxFF makes it uniquely applicable for both metallic and covalent systems. Thus, ReaxFF has now become a great computational tool to study many reactive systems; at the same time, it has enabled researchers throughout the world to investigate previously inaccessible computational chemistry problems. Apart from studying combustion problems, ReaxFF method has been extensively used to investigate a wide range of applications in materials [45–50] catalysts [51, 52], and other chemical systems [53–57].

Combustion, being a complex reactive system, requires an atomistic-level understanding of the intricate details regarding the underlying reactions and species to facilitate better engine and fuel design. To this end, the first ReaxFF combustion force field (CHO-2008) was developed by Chenoweth et al. [24] in 2008. Since then, it has been implemented in a wide range of applications in scientific community for studying pyrolysis and oxidation of variety of fuels, for example, JP-10 [25] n-dodecane [58], 1-heptane [30], n-octanol [29], toluene [59], Illinois no. 6 coal [26], 1,6-dicyclopropane-2,4-hexyne [60] and liginin [61], and many more. The recent development of GPU-enabled ReaxFF [62] has made it suitable to simulate large complex systems like coal [63] and lignin [64] pyrolysis. Apart from the hydrocarbon fuel, this description has also been used to investigate a wide range of aspects related to carbon-based materials including the oxidation of graphene [65], structural and chemical properties of graphene oxide [66], chemomechanics of crack propagation in graphene [67] and dynamics of carbon nano-onion formation [68]. For a more detailed review of this force field, we refer to the recent paper by Dontgen et al. [31].

Though ReaxFF CHO-2008 description was very good in describing the initial pyrolysis and oxidation of large hydrocarbons, where the initial combustion process

is mainly dominated by the pyrolysis process, it failed to describe the chemistry of smaller hydrocarbon properly [28]. Additionally, CHO-2008 parameter set was not transferable to study mechanical properties of condensed phase carbons [69]. Furthermore, the O_2 in CHO-2008 description is highly reactive, which can abstract H from hydrocarbon chain at a faster-than-expected rate. This might send us a false alarm of system initiation during the simulation. Srinivasan et al. [69] derived an improved set of ReaxFF carbon parameters for describing carbon-condensed phases and taking those parameters on board, Ashraf et al. [28] have recently published an extended version of ReaxFF combustion force field (CHO-2016), which addresses the limitations of CHO-2008 description while retaining the overall quality of CHO-2008 description for larger hydrocarbon combustion. Thus, a single force field can now be used to study not only both the condensed and the gas phase carbon, but also the combustion of any hydrocarbon irrespective of fuel size or structure. This ensures a greater transferability of ReaxFF force field to study any combustion related problems.

Chemical reactions occurring in combustion are considered 'rare events' in MD simulations as not every collision between molecules lead to a reaction. Additionally, reactive MD simulations are expensive as it needs to calculate the bond order at every time step, thus the simulations are limited to only a couple of nano-seconds or less, whereas the timescales associated with combustion reactions at experimental conditions are micro-second-level phenomenon. MD simulations are thus typically carried out at high temperatures and pressures to accelerate the system dynamics and capture the appropriate chemical reactions. Therefore, ReaxFF-based MD simulations are suitable for studying the complex chemistry at high-pressure condition although sometimes the pressure in ReaxFF simulation may exceed the highest possible pressure that a rocket engine can survive. However, despite this shortcoming, it is arguably the most appropriate currently available method to study the high-pressure combustion chemistry. Almost all of the ReaxFF combustion studies mentioned above were performed at very high pressure to study the kinetics of different fuels. Additionally, Ashraf et al. [27] have recently demonstrated that ReaxFF-MD simulations can also be used to study dynamic properties like ignition front speed at supercritical conditions.

In this chapter, we will demonstrate how we can use ReaxFF-MD simulations to calculate Arrhenius parameters for different hydrocarbons at very high pressure and temperature condition. Since the hydrocarbons do not typically exist in a single-component form, we will also investigate how the blending of a highly reactive hydrocarbon with a less reactive one alters the combustion properties of the mixture. This enabled us to identify pressure/temperature and mixing conditions, where the simple first-order kinetics and Arrhenius-type relation fails to prevail, indicating that more complex relationship is required to calculate mixture activation energies. Since experiments are difficult to conduct and measurements are hard to perform at very high pressure/temperature condition, these information from ReaxFF-MD simulation will certainly open up the possibility to study the mixing effects of multiple hydrocarbons at supercritical condition.

7.3 Simulation Details

Since typical transportation fuels used for combustion are highly complex mixture of various hydrocarbons, for modeling purpose, Kim et al. [70] developed two different surrogates for diesel so that various physical and chemical processes inside of a diesel engine can be replicated. The surrogate fuels are either a mixture of n-dodecane/*iso*-cetane/methylcyclohexane/toluene or a mixture of n-dodecane/*iso*-cetane/decalin/toluene, where n-dodecane is the most reactive one and toluene is the least. As such, for our study, we decided to investigate the effect of n-dodecane addition on toluene pyrolysis using the reactive molecular dynamics (RMD) simulations. We also used two different densities for the overall system, to investigate the effect of density/pressure on the pyrolysis of the mixtures. All of the MD simulations in this section were performed employing the ReaxFF method with a constant number of atoms (N) in a constant volume (V) while keeping the temperature constant (T) using a thermostat, as described by the NVT-MD ensemble. Also, we used the recently developed combustion force field by Ashraf et al. [28] in this study.

7.3.1 Single-Component System

First, to determine the applicability of the force field, toluene and n-dodecane pyrolysis have been investigated independently using homogeneous system. We placed 40 toluene molecules in two cubic periodic unit boxes of dimension 31.20 Å × 31.20 Å × 31.20 Å and 25.00 Å × 25.00 Å × 25.00 Å, where the overall system densities are 0.2 kg/dm^3 and 0.4 kg/dm^3 respectively. Similarly, in case of n-dodecane, we placed 40 molecules in cubic boxes of dimension 38.39 Å × 38.39 Å × 38.39 Å and 30.47 Å × 30.47 Å × 30.47 Å, respectively, to generate systems of similar densities like toluene. Next, each system is energy minimized and equilibrated using NVT simulation for 10 ps at a temperature of 1500 K. Test cases has been run beforehand to ensure that no thermal decomposition occurs at this temperature for both toluene and n-dodecane. After equilibration, 10 different initial configurations of the system were selected to perform a series of NVT-MD simulations. For each case, the system temperature was varied from 2000 to 2600 K at 100 K interval. The average initial pressure of the system for the first 5 ps of the NVT-MD simulations was in the range of 26–75 MPa. Although the use of such high temperatures and pressures is rarely seen in experiments, this is essential in MD simulations to keep the computational time within a reasonable scope. The high temperature and subsequent high pressure results in a larger number of collisions in the system and thereby reduces the reaction time (Fig. 7.2).

During all of the simulations, the time step has been kept as 0.1 fs, which is appropriate for describing hydrocarbon reaction mechanism at high temperatures [24]. Since n-dodecane is highly reactive, a simulation time of 50 ps was enough to calculate the Arrhenius parameters. On the other hand, the toluene simulations

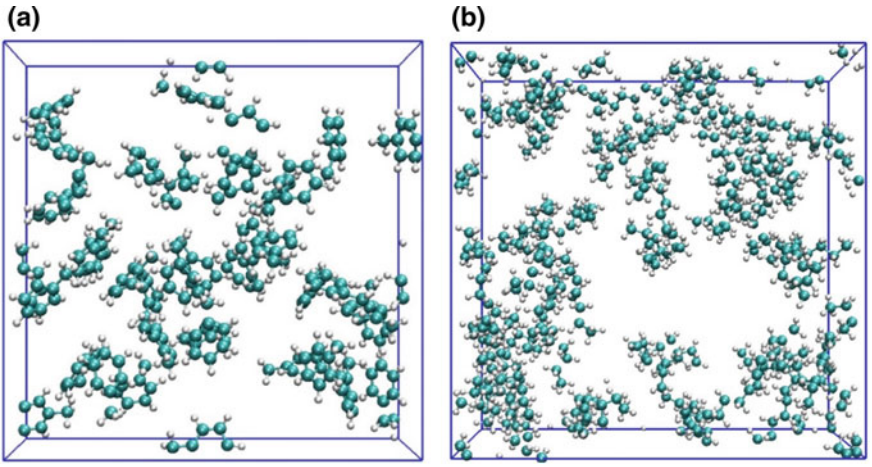

Fig. 7.2 Snapshots of representative single-component system of equilibrated **a** toluene, and **b** n-dodecane with density of 0.2 kg/dm^3. The carbon and hydrogen atoms are displayed in cyan and white, respectively

were run for 200 ps due to the less reactive nature of toluene. The results from the simulations with 10 different starting configurations were then averaged to obtain the reactant decomposition and overall product distribution. This information is then used to get the Arrhenius parameters for individual components.

7.3.2 n-*Dodecane and Toluene Mixture (Multicomponent System)*

Once we validated the quality of the force field against the single-component system, we moved on to explore the effect of n-dodecane presence to the pyrolysis of toluene at high-pressure/temperature condition which is the main focus of this chapter. To do this, we performed a series of NVT-MD simulations of toluene and *n*-dodecane mixtures, where these two hydrocarbons are introduced in different ratios. Table 7.1 represents a summary of all the input configurations for these systems.

All of the systems studied were equilibrated using NVT-MD after placement of the molecules at a temperature of 1500 K for 10 ps. Then, 10 different initial configurations of the molecules were generated and a series of NVT-MD simulation at temperatures 2000, 2100, 2200, 2300, 2400, 2500, 2600 K were carried out for all of them. The total simulation time was 200 ps with the time step being 0.1 fs. We repeated all the simulations changing the system density to 0.4 kg/dm^3 to study and compare the effect of a higher density/pressure of the system.

For all the simulations, whether single-component or multicomponent, the following parameters were the same. To keep the system temperature constant, the

Table 7.1 Initial configurations of different *n*-dodecane and toluene mixtures

n-Dodecane: Toluene	% of n-dodecane in the mixture	Density (kg/dm^3)	Temperature range (interval)	Box dimension
1:40	2.44	0.2	2000 K–2600 K (100 K)	31.75 Å × 31.75 Å × 31.75 Å
5:40	11.11	0.2	2000 K–2600 K (100 K)	33.52 Å × 33.52 Å × 33.52 Å
10:40	20.00	0.2	2000 K–2600 K (100 K)	35.50 Å × 35.50 Å × 35.50 Å
20:40	33.33	0.2	2000 K–2600 K (100 K)	38.91 Å × 38.91 Å × 38.91 Å
40:40	50.00	0.2	2000 K–2600 K (100 K)	44.34 Å × 44.34 Å × 44.34 Å

temperature was controlled by the Berendsen thermostat using a temperature damping constant of 100.0 fs. For molecular recognition, we used a bond-order cut off of 0.3. The choice of bond-order cutoff does not alter the simulation pathway, but it is only used to identify the intermediates and products formed during the MD simulations.

7.3.3 Continuum Simulations

In addition to the ReaxFF-based simulations described above, zero-dimensional (time-evolving), continuum-scale pyrolysis simulations of the same series of test cases (see Table 7.1) are performed. The intent is to highlight the deficiency of Arrhenius-type chemical kinetics in predicting chemical evolutions (e.g., pyrolysis) under high-pressure high temperature conditions, by comparing the results obtained from both approaches. For this purpose, the initial temperatures, density, and mole fractions of n-dodecane and toluene in these continuum simulations are set to be the same as those used in the molecular dynamics simulations as described in Table 7.1, and these simulations are performed with constant volume and constant temperature to best duplicate the same running conditions as for the ReaxFF simulations. In these simulations, a cubic equation of state is used to account for real gas effects [71], and a widely used chemical kinetic mechanism [27] with Arrhenius-type rate coefficients is used. This chemical mechanism contains 179 species and 1895 chemical reactions (forward and backward reactions counted separately), and it has been extensively validated for jet fuel surrogate components under lower pressure and temperature ranges (up to 40 bars and 1250 K) [72].

7.4 Results and Discussion

7.4.1 *Kinetic Analysis of Toluene and n-Dodecane Pyrolysis as Single-Component System*

For single-component systems of toluene and n-dodecane, first-order kinetics has been used to study the thermal decomposition. We used the consumption rate from the ReaxFF-MD simulations in this analysis and the number of reactant molecules has been chosen to represent the reactant concentration. From the NVT-MD simulations at different temperatures, the decomposition of toluene and n-dodecane has been found to change as a function of time and temperature. Using this information, we used integrated first-order rate law to determine the rate constant at each temperature:

$$\ln(N_0) - \ln(N_t) = \mathrm{kt} \tag{7.2}$$

where N_0 is the number of molecules initially in the system and N_t is the number of molecules at any time t. At each temperature, the quantity $\ln(N_0) - \ln(N_t)$ has been plotted against time and the rate constant has been determined from the slope of the linear fitting of the plot. We used these rate constants from different temperatures in the Arrhenius plot of toluene and n-dodecane as shown in Fig. 7.3. The activation energy (E_a) and the pre-exponential factor (A) were calculated with the help of a linear fit of the plot and the Arrhenius equation described as

$$k = A \exp(-E_a/\mathrm{RT}) \tag{7.3}$$

Next, we compared the values of Arrhenius parameters obtained from ReaxFF-MD simulations with their experimental counterparts, which are listed in Table 7.2.

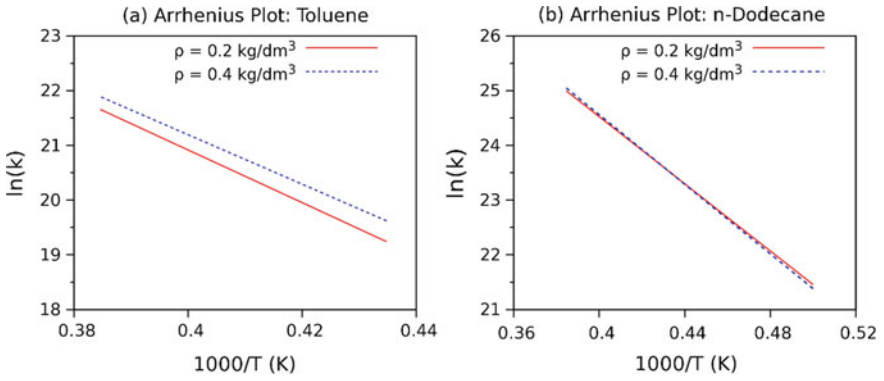

Fig. 7.3 Arrhenius plot for calculated and fitted rate constants of **a** toluene, **b** n-dodecane as single-component systems with density $\rho = 0.2$ and 0.4 kg/dm^3

Table 7.2 Fitted Arrhenius equation and parameters for n-dodecane and toluene

Molecule	ReaxFF			Experiment [73, 74]	
	Density (kg/dm^3)	E_a (kcal/mol)	A (1/s)	E_a (kcal/mol)	A (1/s)
Toluene	0.2	95.71	28.3×10^{16}	88.9–97.0	$0.28 - 1 \times 10^{16}$
	0.4	89.90	11.59×10^{16}		
n-Dodecane	0.2	60.94	0.95×10^{16}	61.32	0.12×10^{16}
	0.4	63.11	1.53×10^{16}		

It is important to note that, the experimental values are obtained at a much lower pressure and temperature condition than ReaxFF simulations. For example, Colket et al. [73] investigated the pyrolysis of toluene at a temperature range of 1200–1850 K with a total pressure of approximately 1 MPa. According to them, the formation of benzyl radical is the most dominant reaction pathway, which is also accompanied by the pathway that leads to phenyl radical formation. The activation energies mentioned in Table 7.2 are for these two key reaction pathways.

Liu et al. [74] investigated the supercritical thermal cracking of n-dodecane at a temperature range 700–800 K and pressure of 3–4 MPa. For both toluene and n-dodecane, the results obtained in this work shows good agreement with those obtained from the experiments. Wang et al. [58] investigated the pyrolysis of n-dodecane using ReaxFF-MD simulations and the force field parameters developed by Chenoweth et al. [24] using a temperature range of 2100–3000 K. The activation energies of n-dodecane derived in the study were 63.68 and 66.14 kcal/mol for densities $\rho = 0.17$ and 0.33 kg/dm^3. The activation energy of n-dodecane derived in this work using the recently developed force field by Ashraf et al. [28] showed a better agreement with the experimental results than those derived by Wang et al. [58] using Chenoweth et al. [24] force field. Though in our simulations pressure and temperature are much higher than their experimental counterparts, the reasonable agreement with experimental values indicates that the simple Arrhenius type relation holds good for single-component system, even at a very high pressure and temperature.

Figure 7.4 shows the evolution of toluene and dodecane molecules as a function of time for both of the densities 0.2 and 0.4 kg/dm^3. At temperatures 2000, 2100, and 2200 K, the number of toluene decomposed was very low, so the simulation results are not used in calculations of the Arrhenius parameters since these would include a significant statistical uncertainty. The figures indicate the reactivity of n-dodecane as opposed to that of toluene. We observed that at 2000 K, n-dodecane began to decompose within 5 ps of the simulation time; at temperatures higher than 2000 K the decomposition began in less than 5 ps. While in the case of toluene, at temperatures 2300, 2400, and 2500 K, the decomposition does not begin before 20 ps. Only at a high temperature of 2600 K, toluene starts to decompose within 5 ps of the simulation time. The trend of decomposition initiation is observed in both 0.2 and 0.4 kg/dm^3 density cases.

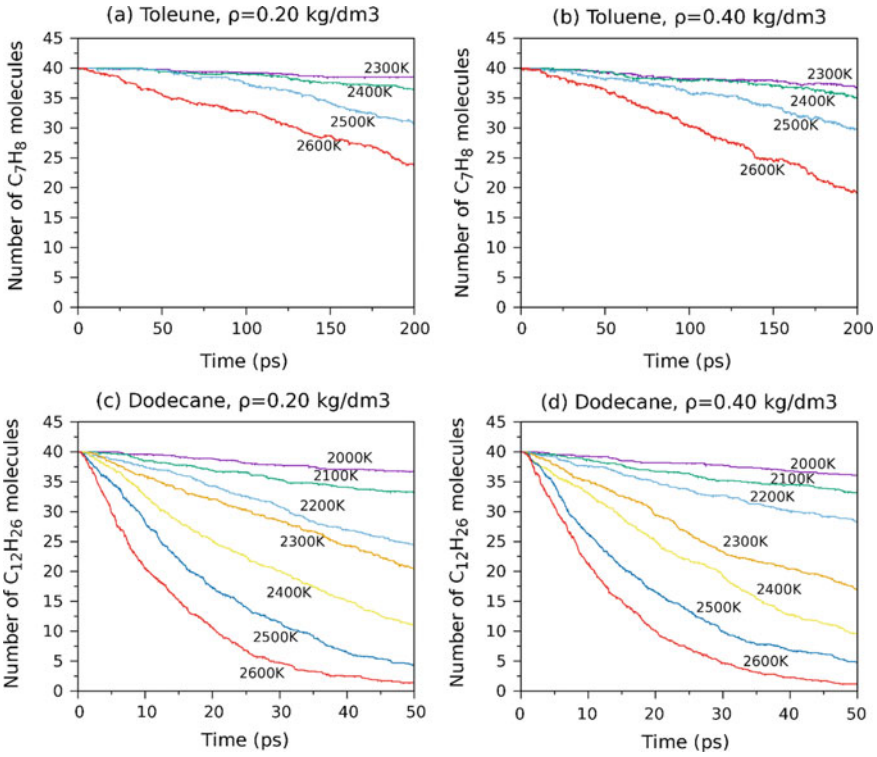

Fig. 7.4 Time evolution of the number of toluene molecules in single-component systems with density **a** $\rho = 0.2$ kg/dm^3 and **b** 0.4 kg/dm^3, and n-dodecane molecules in single-component systems with density **c** $\rho = 0.2$ kg/dm^3 and **d** 0.4 kg/dm^3

As mentioned above, experimentally, the initiation mechanism for toluene pyrolysis is dominated by decomposition of toluene into benzyl (C_7H_7) and hydrogen atom with activation energy 88.9 kcal/mol [71]. The hydrogen atom generated from this toluene decomposition reacts with another toluene molecule to produce another benzyl radical and hydrogen molecule. Another reaction pathway is the formation of phenyl (C_6H_5) and methyl radical (CH_3). A similar initiation mechanism is observed in ReaxFF simulations shown in Scheme 7.1a. Figure 7.5a demonstrates the distribution of toluene and its major decomposition species at 2600 K. The decomposition of toluene starting after 10 ps is on the rise accompanied by a gradual rise of both benzyl and hydrogen molecule.

The pyrolysis of n-dodecane is dominated by radical production in ReaxFF as shown in Fig. 7.5b. This is in agreement with experiment [75]. The initiation reactions principally involve C–C bond fission to produce two alkyl radicals as shown in

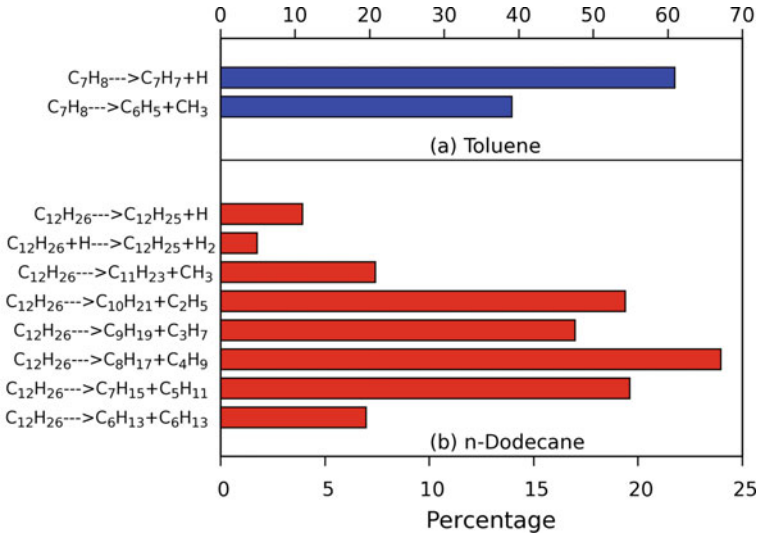

Scheme 7.1 Initiation reaction mechanism and their relative percentages occurred in **a** toluene, **b** n-dodecane pyrolysis in a single-component system revealed by ReaxFF–MD simulations at 2600 K

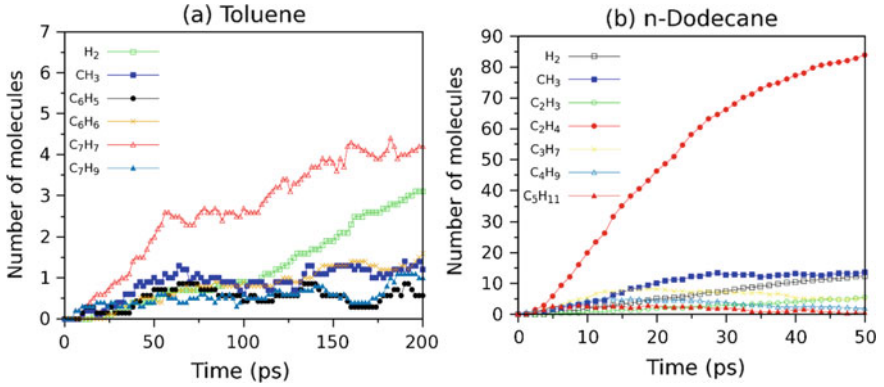

Fig. 7.5 Time evolution of the major species generated in the pyrolysis of **a** toluene, **b** n-dodecane in single-component systems with density $\rho = 0.2$ kg/dm^3 and temperature $T = 2600$ K

Scheme 7.1b. On rare occasion, we observe abstraction of hydrogen from n-dodecane. As the simulation proceeds, larger alkyl radicals undergo further decomposition, which increases the number of smaller radicals such as CH_3, C_2H_5, C_3H_7 and creates hydrogen molecules and stable double-bond-containing molecules like C_2H_4 and C_3H_6.

7.4.2 *Pyrolysis of Toluene and* n-*Dodecane as Multicomponent System*

7.4.2.1 Kinetic Analysis

To investigate the change in activation energy of a less reactive fuel component due to the presence of a more reactive molecule, we analyzed a multicomponent system of n-dodecane and toluene using ReaxFF NVT-MD simulations. The rate constants associated with the decomposition of toluene in the mixture are determined using the first-order kinetics and the number of toluene molecules in (7.3). We derived the Arrhenius parameters in (7.3) from the fitted plot of these rate constants at various temperatures.

Figure 7.6 shows the activation energies (E_a) of toluene in the mixtures as a function of the percentage of n-dodecane introduced in the mixture for both ReaxFF-MD and continuum simulations. The zero-percentage result indicates the pyrolysis of toluene as a single component. As the percentage of n-dodecane increases, the activation energy of toluene decreases rapidly. According to ReaxFF-MD results, the presence of a single n-dodecane molecule during the thermal decomposition of toluene reduces the activation energy from 95.69 to 81.68 kcal/mol (14.64% reduction). If n-dodecane molecule number is increased to 5, the activation energy reduces further to 66.78 kcal/mol. When the percentage of n-dodecane is 33.33 in the mixture (n-dodecane and toluene ratio 20:40) we see that the activation energy of toluene (52.98 kcal/mol) even drops below that of single-component n-dodecane pyrolysis (52.98 kcal/mol) with the same density. The results from continuum simulations show similar behavior. Both set of results show good qualitative agreement in predicting the mixture activation energy, when the n-dodecane concentration is low (less than 20%). This suggests the capability of ReaxFF-MD to predict the activation energy of toluene within this mixing ratio. However, the results show larger deviations when n-dodecane concentration is higher than 20%. Unlike ReaxFF-MD, the activation energy of toluene from continuum simulation in all of the mixtures remains higher than n-dodecane only system. This indicates that with the presence of higher amount of n-dodecane, the first-order kinetics-based Arrhenius method fails to predict the mixture activation energy with sufficient accuracy.

7.4.2.2 Effect of Toluene Presence on the Pyrolysis of *n*-Dodecane

Before investigating what is causing the dramatic decrease of activation energy of toluene at the presence of n-dodecane, we want to check if the presence of toluene also affects the activation energy of n-dodecane. To get an overview, here we have compared the single-component system of n-dodecane and the mixture of 40 toluene and 40 n-dodecane molecules. The rate constants were determined in this case using (7.3) and the time evolution of only n-dodecane molecules in the mixture. We calculated the activation energy similarly using (7.3) and the linear fitting of Arrhenius plot

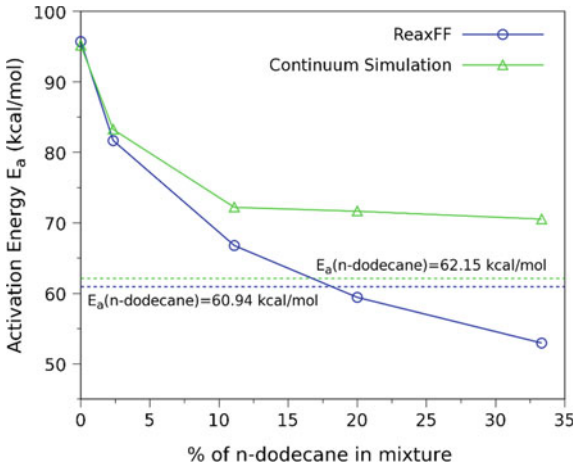

Fig. 7.6 Activation energies of toluene at various compositions of n-dodecane and toluene mixture from ReaxFF-MD simulations and Continuum simulations. The green and blue dashed line represents the activation energy of n-dodecane calculated by ReaxFF and Continuum simulations, respectively

of rate constants at different temperatures. The value of activation energy is found to be 58.56 kcal/mol, which is very close to the activation energy 60.94 kcal/mol found in Sect. 7.4.1. Since the activation energy of n-dodecane in the mixture is close to that obtained from individual n-dodecane system, we can conclude the pyrolysis of n-dodecane is mostly independent of the presence of toluene.

Figure 7.7 shows the time evolution of n-dodecane molecules in both single-component system and a 40:40 mixture of toluene and n-dodecane at 2300 K and at 2600 K. The time-dependent number of n-dodecane molecules in the system is averaged from 10 different NVT-MD simulations of the same system but with different initial configurations. The simulation time of n-dodecane in extended to 100 ps to get a better comparison of n-dodecane decomposition. The figures indicate that there is no significant change in the pyrolysis of n-dodecane even though the two systems are different. We can conclude from these results that the initiation mechanism of n-dodecane pyrolysis is mostly independent and is not affected by the presence of a less reactive fuel like toluene.

7.4.2.3 Effect of n-Dodecane Presence on the Pyrolysis of Toluene

Although the pyrolysis of n-dodecane is mostly unaffected by the presence of toluene in the mixture, this is not the case for toluene itself. Figure 7.8 shows the number of toluene molecules decomposed in the single-component system and the mixtures with different concentrations of n-dodecane for a total simulation time of 200 ps.

A preliminary analysis of the product distribution observed during the decomposition of toluene at temperatures from 2000 to 2600 K shows that as the number of n-dodecane in increased in the mixture, the number of toluene decomposed also increases, even as the number of toluene molecules introduced initially is constant (40). This indicates the existence of several simultaneous processes during the ther-

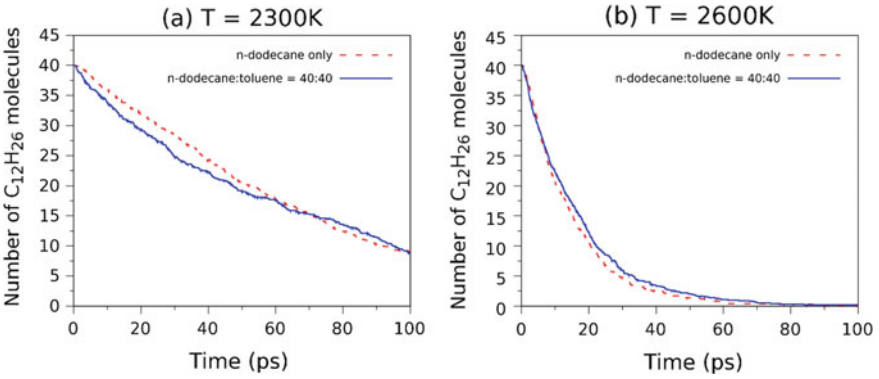

Fig. 7.7 Time evolution the numbers of n-dodecane molecules at temperatures **a** $T = 2300$ K and **b** $T = 2600$ K

mal decomposition of toluene. At low temperatures, since the decomposition of toluene in single-component system is very low, the role of n-dodecane plays a much more significant role in further decomposition of toluene.

The Arrhenius plots for the pyrolysis simulations of toluene and n-dodecane mixtures with increasing concentration of n-dodecane is shown in Fig. 7.9. According to this, at high temperature (2500, 2600 K) the rate constant has been mostly unaffected by the inclusion of n-dodecane in the mixture. However, at low temperatures (2000, 2100, 2200, 2300, 2400 K) the rate constants gradually increase with increasing number of n-dodecane in the mixture. The result is an overall upward shift of the Arrhenius plot at lower temperatures. Additionally, with the increase of n-dodecane molecules in the system, lower temperatures become accessible to calculate the rate constants. For example, in toluene-only case, enough toluene was not decomposed to calculate a rate constant at 2200 K, however, with the presence of n-dodecane, we were able to calculate rate constant even at 2000 K. Thus, the decrease in the slope of the plot which gives the value of—E_a/R implies lower activation energies for increasing n-dodecane number in the mixture.

Though further investigation is required, the different mechanism of toluene and n-dodecane pyrolysis as single-component systems might explain the underlying mechanism responsible for lowering the activation energies of the mixture. Figure 7.4 shows that, at lower temperature (2000 K), roughly 15% of n-dodecane molecules decompose within the 50 ps simulation time of n-dodecane only system, while it reaches to over 90% at higher temperature (2600 K). The decomposition behavior of n-dodecane is observed in the mixtures too; the process is accompanied by the production of a large radical pool. The main species in the radical pool consists of a combination of different alkyl radicals ranging from C_1–C_{12} initially and smaller radicals such as methyl (CH_3), ethyl (C_2H_5), propyl (C_3H_7) and in the later part of the simulation, hydrogen (H) radical etc. At low temperatures, the intramolecular reaction between the small free radicals and toluene molecules cause further decomposition of toluene into benzyl radical (C_7H_7) and H. For example, the reaction

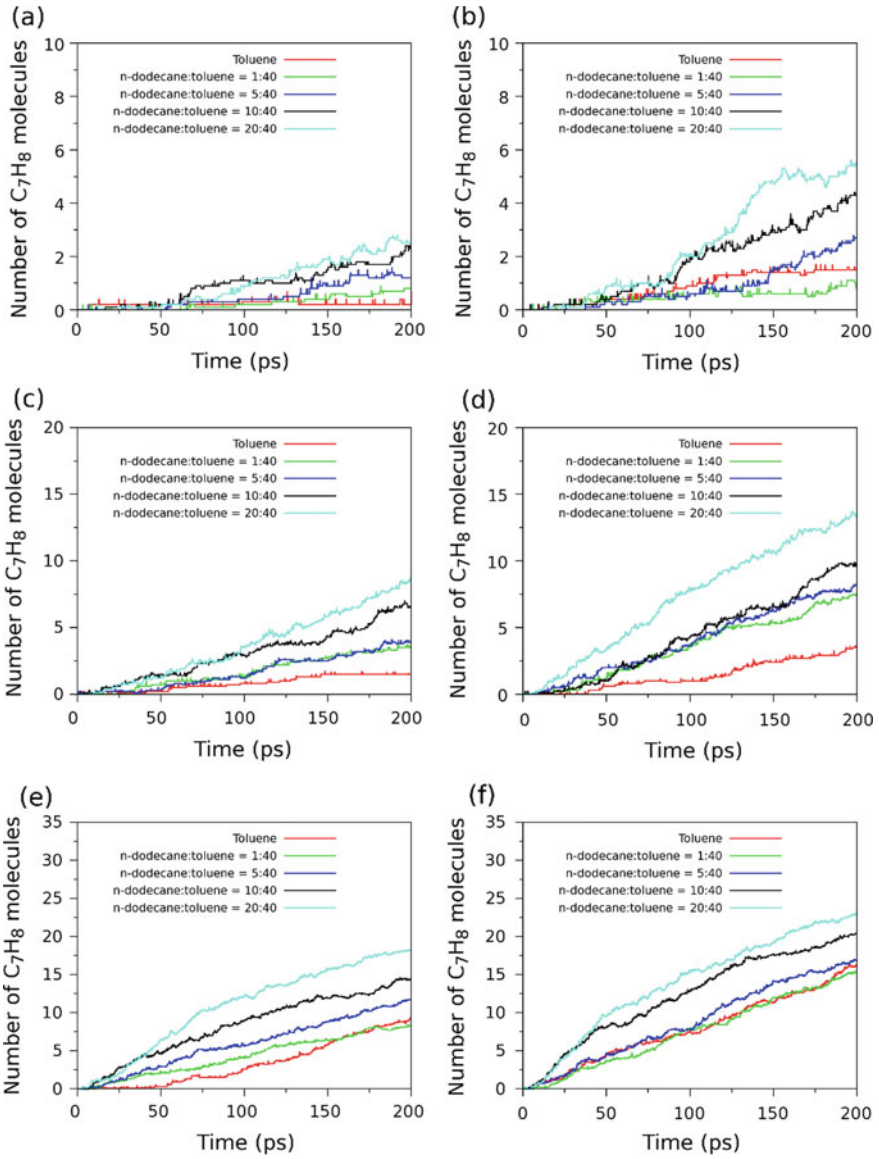

Fig. 7.8 Time evolution the numbers of toluene molecules for single-component system and in mixtures with various concentrations of n-dodecane at temperatures **a** $T = 2100$ K, **b** $T = 2200$ K, **c** $T = 2300$ K, **d** $T = 2400$ K, **e** $T = 2500$ K, and **f** $T = 2600$ K

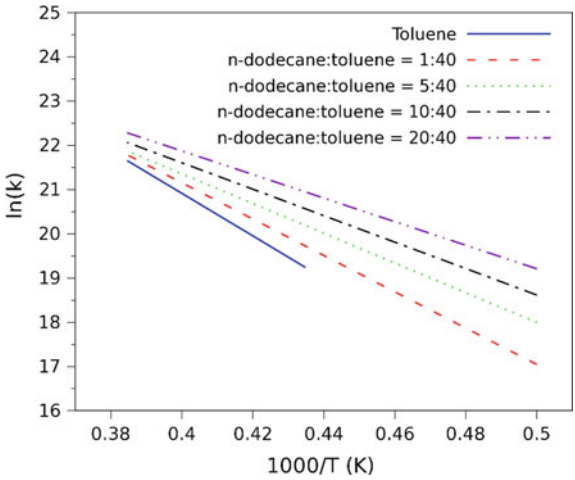

Fig. 7.9 Arrhenius plot with the fitted natural logarithm of rate constant versus the inverse of temperature for toluene as single-component system and in mixtures with various concentrations of n-dodecane at densities of $\rho = 0.2$ kg/dm^3

between methyl (CH_3) and toluene (C_7H_8) to generate methane (CH_4) and benzyl has an energy barrier of only 11.1 kcal/mol [70]. With the presence of n-dodecane, such reactions with low barriers cause further decomposition of toluene in a shorter time.

7.4.2.4 Density/Pressure Effect on the Pyrolysis of Toluene and n-Dodecane Mixture

To investigate the density/pressure effect on the pyrolysis of toluene and n-dodecane mixture we performed additional simulations for the systems with a high density of 0.4 kg/dm^3. The rate constants and the Arrhenius parameters are calculated based on toluene using the same method in Sect. 7.4.1. Figure 7.10a shows the comparison of the activation energies from ReaxFF simulations for density 0.2 and 0.4 kg/dm^3 with increasing percentage of n-dodecane in the mixture. Overall, the results show that the activation energy for a system density of 0.4 kg/dm^3 is less than that for a system density of 0.2 kg/dm^3 when the percentage of n-dodecane is low in the mixture (2.34 and 11.11%). For 10 and 20 molecules of n-dodecane in the mixture, the density/pressure effect is insignificant and the activation energies for both cases are almost similar. For the high density case, we observe that the presence of only 11.11% n-dodecane in the mixture results in a surprisingly lower activation energy of toluene than that of n-dodecane as a single-component system. Figure 7.10b shows results for similar cases obtained through continuum-scale pyrolysis simulations. At higher density, the activation energy of toluene decreases sharply from 95.17 to just 62.79 kcal/mol (34%) with the addition of only one n-dodecane molecule in the toluene-only system. After that, the activation energy keeps on increasing as the percentage of n-dodecane increases. Similar to ReaxFF-Md results, when n-dodecane number in the mixture is 10 and 20, the results are very similar for the

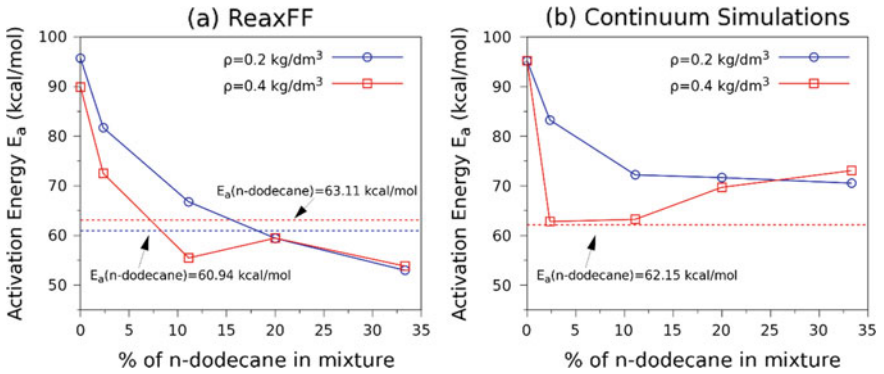

Fig. 7.10 Activation energies of toluene at various compositions of n-dodecane and toluene mixture from **a** ReaxFF-MD simulations. **b** Continuum simulations with two different densities. The blue and red dashed line represents the activation energy of only n-dodecane in a system density of 0.2 kg/dm^3 and 0.4 kg/dm^3, respectively

two density cases. These results are in qualitative agreement with the ReaxFF-MD results in the sense that at higher concentrations of n-dodecane in the mixture, the toluene activation energy does not show any dependency on either the amount of n-dodecane in the mixture or the overall system density.

These ReaxFF-MD results indicate that apparent first-order kinetics is no longer suitable for calculation of activation energy of toluene in the mixture at high density/high pressure system. We can also conclude that when the ratio of n-dodecane and toluene exceeds a certain threshold (in our case more than 5:40), the method has limitations in accurately capturing the effect of the n-dodecane in the activation energy of toluene. It is evident from the results that the decomposition of toluene follows a more complex mechanism in the mixture in high density/pressure than in low density/pressure. Therefore, in order to determine the activation energy of a less reactive component such as toluene in a mixture with a highly reactive molecule such as n-dodecane, we need to look beyond the simple first-order kinetics and the Arrhenius equation.

A complete investigation of this surprising behavior of toluene decomposition with the presence of n-dodecane is beyond the scope of this study, as the purpose of this book chapter is to demonstrate the capability of ReaxFF-MD simulation for high pressure/temperature combustion. However, we would like to propose a hypothesis for this interesting finding, which requires more rigorous studies to confirm. According to our hypothesis, the main reason for low activation energy of toluene in the presence of n-dodecane is mostly related to the very different initiation mechanism of toluene and n-dodecane decomposition, when they are studied as a single-component system. As mentioned several times in this work, n-dodecane decomposition leads to a large alkyl radical pool build up, and at high density, these radicals can easily find a toluene molecule to decompose as they are diffusion limited at that density. Since n-dodecane can generate radicals even at lower temperatures, this leads to higher

toluene decomposition, which significantly effects toluene activation energy. That is why, a small amount of n-dodecane can significantly reduce toluene activation energy when simple first-order kinetics and pressure-independent Arrhenius equation is used at high density (0.4 kg/dm^3). However, at a relatively lower density such as 0.2 kg/dm^3 and lower number of n-dodecane in the system, active alkyl radicals has more space to move around and it takes longer time for them to find a toluene molecule to collide with as the alkyl pool build up is not that significant. However, even at low density, simple Arrhenius equation is not applicable if the initial number of n-dodecane is high as it significantly increases the number of alkyl radicals in the system. Since we used first-order kinetics to calculate the rate constant, while the toluene decomposition is mostly the secondary reaction in the system initiated by active radicals, our analysis no longer holds at this situation.

Additionally, we hypothesize that, at higher temperatures, toluene decomposition shows more temperature dependence than density/pressure dependence. Also, at high temperature, the presence of n-dodecane does not greatly affect the rate constant of toluene which is supported in Fig. 7.9 too. At higher temperatures, probably toluene in mixture decomposes in a similar manner as the toluene-only system as those high energy decomposition routes become accessible. As these routes no longer require an effective collision, toluene mainly decomposes in those routes.

As mentioned above, our hypothesis requires further investigation to confirm, however, with the aid of ReaxFF-MD simulation we were able to gain some useful information of high pressure system, which was never explored before.

7.5 Conclusions

In this work, we applied ReaxFF method to study the pyrolysis of toluene and n-dodecane as both single-component systems and mixtures subjected to high temperature and pressure conditions. A series of NVT-MD simulations for a temperature range of 2000–2600 K has been performed to investigate the decomposition of the reactant molecules and to calculate the temperature-dependent rate constants. Two different densities, 0.2 and 0.4 kg/dm^3 of the system were used to investigate the effect of a higher density/pressure on the Arrhenius parameters. First-order kinetics was used to calculate the Arrhenius parameters based on the toluene decomposition and corresponding rate constants calculated at different temperatures. In case of mixtures of toluene and n-dodecane, zero-dimensional (time-evolving) continuum-scale pyrolysis simulations for the same tests cases have been performed and the results were then compared to those obtained from ReaxFF-MD.

For individual systems of toluene and n-dodecane, the activation energy and the pre-exponential factor calculated in both high- and low-density cases show good agreement with previous experimental results. For mixtures having relatively lower density (0.2 kg/dm^3) of the system, we observed from both of the methods that the overall effect of n-dodecane is to reduce the activation energy of toluene. The two methods showed satisfactory correlation when the n-dodecane concentration

is below 20%. Overall, for all the cases the two methods showed good qualitative agreement. In addition, we observed that as the percentage of n-dodecane in the mixture is increased beyond a threshold value (in our case >11.11%), the ReaxFF-MD simulations predict an activation energy even lower than that of n-dodecane in single-component system. This suggests that the pyrolysis of toluene follows a much more complex mechanism in the presence of a greater concentration of n-dodecane. In this case, the simple Arrhenius relation based on first-order kinetics does not hold anymore to accurately predict the activation energy of toluene. A preliminary investigation of the time evolution of major species generated by n-dodecane showed that the pyrolysis of n-dodecane is radical dominated. The large alkyl radical pool generated by the thermal decomposition of n-dodecane are highly reactive and they cause further dissociation of toluene. This played a critical role in low temperatures especially, since at low temperatures the toluene decomposition by itself is very limited.

In the higher density case (0.4 kg/dm^3) even small amounts of n-dodecane had much more significant impact on the decomposition of toluene and its activation energy. This was observed in both ReaxFF-MD and continuum simulation results. Beyond a certain mixture ratio, the activation energy did not show any dependence on the number of n-dodecane in the mixture or the overall system density. We hypothesize that a different initiation mechanism is at work in these cases, which needs further studies to be confirmed.

These results demonstrate that although ReaxFF-MD is useful in determining the Arrhenius parameters for single-component systems, in case of mixtures the same methodology only applies in certain cases of densities and mixture ratios. This is also confirmed using the results of continuum-scale pyrolysis simulations. When the overall system density/pressure is high or the concentration of a highly reactive molecule in the mixture is increased, the simple first-order kinetics-based Arrhenius equation does not apply. We need to look further into the complex reaction pathways to determine the effective mixture activation energies in these cases.

Acknowledgements CA, SS and ACTvD acknowledge funding from AFOSR FA9550-17-1-0173.

References

1. Sutton GP (2006) History of liquid propellant rocket engines. AIAA
2. Poling BE, Prausnitz JM, O'connell JP et al (2001) The properties of gases and liquids, vol 5. Mcgraw-hill, New York
3. Bianchi GM, Pelloni P, Corcione FE, Allocca L, Luppino F (2001) Modeling atomization of high-pressure diesel sprays. J Eng Gas Turbines Power 123(2):419–427
4. A validated numerical simulation of diesel injector flow using a VOF method. http://papers.sae.org/2000-01-2932/. Accessed 22 May 2017
5. Gnanaskandan A, Bellan J (2017) Numerical simulation of jet injection and species mixing under high-pressure conditions. J Phys: Conf Ser 821(1):012020
6. Falgout Z, Rahm M, Wang Z, Linne M (2015) Evidence for supercritical mixing layers in the ECN spray A. Proc Combust Inst 35(2):1579–1586

7. Mayer W, Telaar J, Branam R, Schneider G, Hussong J (2003) Raman measurements of cryogenic injection at supercritical pressure. Heat Mass Transf 39(8–9):709–719
8. Oschwald M, Schik A, Klar M, Mayer W (1999) Investigation of coaxial LN2/GH2-injection at supercritical pressure by spontaneous Raman scattering. 35th Joint propulsion conference and exhibit, p 2887
9. Oschwald M, Schik A (1999) Supercritical nitrogen free jet investigated by spontaneous Raman scattering. Exp Fluids 27(6):497–506
10. Roy A, Joly C, Segal C (2013) Disintegrating supercritical jets in a subcritical environment. J Fluid Mech 717:193–202
11. Roy A, Segal C (2010) Experimental study of fluid jet mixing at supercritical conditions. J Propuls Power 26(6):1205–1211
12. Segal C, Polikhov SA (2008) Subcritical to supercritical mixing. Phys Fluids 20(5):052101
13. Falgout Z, Rahm M, Sedarsky D, Linne M (2016) Gas/fuel jet interfaces under high pressures and temperatures. Fuel 168:14–21
14. Manin J, Pickett LM, Crua C (2015) Microscopic observation of miscible mixing in sprays at elevated temperatures and pressures. ILASS meeting, Rayleigh, NC
15. Moin P, Mahesh K, Direct numerical simulation: a tool in turbulence research. http://Dx.doi.org/10.1146/annurev.fluid.30.1.539. http://www.annualreviews.org/doi/10.1146/annurev.fluid.30.1.539. Accessed 23 May 2017
16. Masi E, Bellan J, Harstad KG, Okong'o NA (2013) Multi-species turbulent mixing under supercritical-pressure conditions: modelling, direct numerical simulation and analysis revealing species spinodal decomposition. J Fluid Mech 721:578–626
17. Borghesi G, Bellan J (2015) Irreversible entropy production rate in high-pressure turbulent reactive flows. Proc Combust Inst 35(2):1537–1547
18. Bellan J (2017) Direct numerical simulation of a high-pressure turbulent reacting temporal mixing layer. Combust Flame 176:245–262
19. Bellan J (2017) Evaluation of mixture-fraction-based turbulent-reaction-rate model assumptions for high-pressure reactive flows. Combust Flame 179:253–266
20. Foster J, Miller RS (2010) Fundamentals of high pressure combustion. na
21. Detailed chemical kinetic models for the combustion of hydrocarbon fuels. ResearchGate. https://www.researchgate.net/publication/221949556_Detailed_chemical_kinetic_models_for_the_combustion_of_hydrocarbon_fuels. Accessed 23 May 2017
22. Wang L-P, Titov A, McGibbon R, Liu F, Pande VS, Martínez TJ (2014) Discovering chemistry with an ab initio nanoreactor. Nat Chem 6(12):1044–1048
23. van Duin ACT, Dasgupta S, Lorant F, Goddard WA (2001) ReaxFF: a reactive force field for hydrocarbons. J Phys Chem A 105(41):9396–9409
24. Chenoweth K, van Duin ACT, Goddard WA (2008) ReaxFF reactive force field for molecular dynamics simulations of hydrocarbon oxidation. J Phys Chem A 112(5):1040–1053
25. Chenoweth K, van Duin ACT, Dasgupta S, Goddard WA III (2009) Initiation mechanisms and kinetics of pyrolysis and combustion of JP-10 hydrocarbon jet fuel. J Phys Chem A 113(9):1740–1746
26. Castro-Marcano F, Kamat AM, Russo Jr MF, van Duin ACT, Mathews JP (2012) Combustion of an illinois no. 6 coal char simulated using an atomistic char representation and the ReaxFF reactive force field. Combust Flame159(3):1272–1285
27. Ashraf C, Jain A, Xuan Y, van Duin AC (2017) ReaxFF based molecular dynamics simulations of ignition front propagation in hydrocarbon/oxygen mixtures under high temperature and pressure conditions. Phys Chem Chem Phys 19(7):5004–5017
28. Ashraf C, van Duin AC (2017) Extension of the ReaxFF combustion force field towards syngas combustion and initial oxidation kinetics. J Phys Chem A
29. Bharti A, Banerjee T (2016) Reactive force field simulation studies on the combustion behavior of n-octanol. Fuel Process Technol 152:132–139

30. Castro-Marcano F, van Duin ACT (2013) Comparison of thermal and catalytic cracking of 1-heptene from ReaxFF reactive molecular dynamics simulations. Combust Flame 160(4):766–775
31. Döntgen M, Przybylski-Freund M-D, Kröger LC, Kopp WA, Ismail AE, Leonhard K (2015) Automated discovery of reaction pathways, rate constants, and transition states using reactive molecular dynamics simulations. J Chem Theory Comput 11(6):2517–2524
32. Mayo SL, Olafson BD, Goddard WA (1990) Dreiding: a generic force field for molecular simulations. J Phys Chem 94(26):8897–8909
33. Allinger NL, Yuh YH, Lii JH (1989) Molecular mechanics. The MM3 force field for hydrocarbons. 1. J Am Chem Soc 111(23):8551–8566
34. Lii JH, Allinger NL (1989a) Molecular mechanics. The MM3 force field for hydrocarbons. 2. Vibrational frequencies and thermodynamics. J Am Chem Soc 111(23):8566–8575
35. Lii JH, Allinger NL (1989b) Molecular mechanics. The MM3 force field for hydrocarbons. 3. The Van Der Waals' potentials and crystal data for aliphatic and aromatic hydrocarbons. J Am Chem Soc 111(23):8576–8582
36. Allinger NL, Chen K, Lii J-H (1996) An improved force field (MM4) for saturated hydrocarbons. J Comput Chem 17(5–6):642–668
37. Sun H (1998) Compass: an ab initio force-field optimized for condensed-phase applications overview with details on alkane and benzene compounds. J Phys Chem B 102(38):7338–7364
38. Brenner DW (1990) Empirical potential for hydrocarbons for use in simulating the chemical vapor deposition of diamond films. Phys Rev B 42(15):9458–9471
39. Brenner DW, Shenderova OA, Harrison JA, Stuart SJ, Ni B, Sinnott SB (2002) A second-generation reactive empirical bond order (REBO) potential energy expression for hydrocarbons. J Phys: Condens Matter 14(4):783
40. Yu J, Sinnott SB, Phillpot SR (2007) Charge Optimized Many-body Potential For The $\mathrm{Si}/{\mathrm{SiO}}_{2}$ System. Phys. Rev. B 75(8):085311
41. Shan T-R, Devine BD, Hawkins JM, Asthagiri A, Phillpot SR, Sinnott SB (2010) Second-generation Charge-optimized Many-body Potential For $\text{Si}/{\text{SiO}}_{2}$ And Amorphous Silica. Phys Rev B 82(23):235302
42. Nouranian S, Tschopp MA, Gwaltney SR, Baskes MI, Horstemeyer MF (2014) An interatomic potential for saturated hydrocarbons based on the modified embedded-atom method. Phys Chem Chem Phys 16(13):6233
43. Tersoff J (1988) Empirical interatomic potential for carbon, with applications to amorphous carbon. Phys Rev Lett 61(25):2879–2882
44. Mortier WJ, Ghosh SK, Shankar S (1986) Electronegativity-equalization method for the calculation of atomic charges in molecules. J Am Chem Soc 108(15):4315–4320
45. LaBrosse MR, Johnson JK, van Duin ACT (2010) Development of a transferable reactive force field for cobalt. J Phys Chem A 114(18):5855–5861
46. Nomura K, Kalia RK, Nakano A, Vashishta P, van Duin ACT, Goddard WA (2007) Dynamic transition in the structure of an energetic crystal during chemical reactions at shock front prior to detonation. Phys Rev Lett 99(14):148303
47. Ostadhossein A, Cubuk ED, Tritsaris GA, Kaxiras E, Zhang S, van Duin AC (2015) Stress effects on the initial lithiation of crystalline silicon nanowires: reactive molecular dynamics simulations using ReaxFF. Phys Chem Chem Phys 17(5):3832–3840
48. Strachan A, van Duin ACT, Chakraborty D, Dasgupta S, Goddard WA (2003) Shock waves in high-energy materials: the initial chemical events in nitramine RDX. Phys Rev Lett 91(9):098301
49. Wood MA, Cherukara MJ, Kober EM, Strachan A (2015) Ultrafast chemistry under nonequilibrium conditions and the shock to deflagration transition at the nanoscale. J Phys Chem C 119(38):22008–22015
50. Verners O, van Duin ACT (2015) Comparative molecular dynamics study of Fcc–Ni Nanoplate stress corrosion in water. Surf Sci 633:94–101
51. Zou C, Van Duin A (2012) Investigation of complex iron surface catalytic chemistry using the ReaxFF reactive force field method. JOM 64(12):1426–1437

52. Shin YK, Kwak H, Vasenkov AV, Sengupta D, van Duin ACT (2015) Development of a ReaxFF reactive force field for Fe/Cr/O/S and application to oxidation of butane over a pyrite-covered Cr2O3 catalyst. ACS Catal 5(12):7226–7236
53. Hong S, van Duin ACT (2015) Molecular dynamics simulations of the oxidation of aluminum nanoparticles using the ReaxFF reactive force field. J Phys Chem C 119(31):17876–17886
54. Verlackt CCW, Neyts EC, Jacob T, Fantauzzi D, Golkaram M, Shin Y-K et al (2015) Atomic-scale insight into the interactions between hydroxyl radicals and DNA in solution using the ReaxFF reactive force field. New J Phys 17(10):103005
55. Yeon J, van Duin ACT (2016) ReaxFF molecular dynamics simulations of hydroxylation kinetics for amorphous and nano-silica structure, and its relations with atomic strain energy. J Phys Chem C 120(1):305–317
56. Yue D-C, Ma T-B, Hu Y-Z, Yeon J, van Duin AC, Wang H et al (2015) Tribochemical mechanism of amorphous silica asperities in aqueous environment: a reactive molecular dynamics study. Langmuir 31(4):1429–1436
57. Zou C, Shin YK, van Duin ACT, Fang H, Liu Z-K (2015) Molecular dynamics simulations of the effects of vacancies on nickel self-diffusion, oxygen diffusion and oxidation initiation in nickel, using the ReaxFF reactive force field. Acta Mater 83:102–112
58. Wang Q-D, Wang J-B, Li J-Q, Tan N-X, Li X-Y (2011) Reactive molecular dynamics simulation and chemical kinetic modeling of pyrolysis and combustion of n-dodecane. Combust Flame 158(2):217–226
59. Cheng X-M, Wang Q-D, Li J-Q, Wang J-B, Li X-Y (2012) ReaxFF molecular dynamics simulations of oxidation of toluene at high temperatures. J Phys Chem A 116(40):9811–9818
60. Liu L, Bai C, Sun H, Goddard WA (2011) Mechanism and kinetics for the initial steps of pyrolysis and combustion of 1,6-dicyclopropane-2,4-hexyne from ReaxFF reactive dynamics. J Phys Chem A 115(19):4941–4950
61. Beste A (2014) ReaxFF study of the oxidation of lignin model compounds for the most common linkages in softwood in view of carbon fiber production. J Phys Chem A 118(5):803–814
62. Kylasa SB, Aktulga HM, Grama AY (2014) PuReMD-GPU: a reactive molecular dynamics simulation package for GPUs. J Comput Phys 272:343–359
63. Zheng M, Li X, Liu J, Wang Z, Gong X, Guo L et al (2014) Pyrolysis of liulin coal simulated by GPU-based ReaxFF MD with cheminformatics analysis. Energy Fuels 28(1):522–534
64. Zhang T, Li X, Qiao X, Zheng M, Guo L, Song W et al (2016) Initial mechanisms for an overall behavior of lignin pyrolysis through large-scale ReaxFF molecular dynamics simulations. Energy Fuels 30(4):3140–3150
65. Goverapet Srinivasan S, van Duin ACT (2011) Molecular-dynamics-based study of the collisions of hyperthermal atomic oxygen with graphene using the ReaxFF reactive force field. J Phys Chem A 115(46):13269–13280
66. Bagri A, Mattevi C, Acik M, Chabal YJ, Chhowalla M, Shenoy VB (2010) Structural evolution during the reduction of chemically derived graphene oxide. Nat Chem 2(7):581–587
67. Huang X, Yang H, van Duin ACT, Hsia KJ, Zhang S (2012) Chemomechanics control of tearing paths in graphene. Phys Rev B 85(19):195453
68. Ganesh P, Kent PRC, Mochalin V (2011) Formation, characterization, and dynamics of onion-like carbon structures for electrical energy storage from nanodiamonds using reactive force fields. J Appl Phys 110(7):073506
69. Srinivasan SG, van Duin ACT, Ganesh P (2015) Development of a ReaxFF potential for carbon condensed phases and its application to the thermal fragmentation of a large fullerene. J Phys Chem A 119(4):571–580
70. Kim D, Martz J, Violi A (2014) A surrogate for emulating the physical and chemical properties of conventional jet fuel. Combust Flame 161(6):1489–1498
71. Oefelein JC (2006) Mixing and combustion of cryogenic oxygen-hydrogen shear-coaxial jet flames at supercritical pressure. Combust Sci Technol 178(1–3):229–252
72. The Force: CaltechMech. http://www.theforce.caltech.edu/CaltechMech/. Accessed 9 June 2017

73. Colket MB, Seery DJ (1994) Reaction mechanisms for toluene pyrolysis. Symposium (International) on combustion, vol 25. Elsevier, pp 883–891
74. Liu G, Han Y, Wang L, Zhang X, Mi Z (2008) Supercritical thermal cracking of n-dodecane in presence of several initiative additives: products distribution and kinetics. Energy Fuels 22(6):3960–3969
75. Herbinet O, Marquaire P-M, Battin-Leclerc F, Fournet R (2007) Thermal decomposition of n-dodecane: experiments and kinetic modeling. J Anal Appl Pyrolysis 78(2):419–429